WOOD RESEARCH
55 (4): 2010
131-148

MATERIAL REMOVAL ASPECTS AND CUTTING POWER REQUIREMENT OF PROFILE INDEPENDENT WOOD-MOULDING

Yiğit Taşcioğlu
Tobb University of Economics and Technology, Department of Mechanical Engineering, Ankara, Turkey

Mike R. Jackson
Loughborough University, Mechatronics Research Centre Loughborough, Leicestreshire, UK

ABSTRACT

This paper investigates the cutting power requirement for the Profile Independent Wood-Moulding Machine (PIMM). Chip severing phenomena is described and the factors affecting the cutting forces in rotary wood machining are surveyed. The nature of material removal and the influences of PIMM's machining parameters on cutting forces are theoretically investigated. Purpose designed cutting power measurement setup is explained and experiment results are discussed. The findings provide a foundation in the design process of a dedicated cutter for the PIMM in order to achieve optimum production rate.

KEY WORDS: wood moulding, cutting forces, PIMM

INTRODUCTION

The idea of PIMM was first introduced in year 2000 (Jackson et al. 2000). Further design solutions were reported in Taşcıoğlu and Jackson (2004). The PIMM realization test rig was revealed to academics and industrialists of the wood machining community (Taşcıoğlu and Jackson 2005, Jackson and Taşcıoğlu 2007) and received wide acclaim. The aim of this machine is to allow the production of profiled timber components without the use of shaped cutting tools. The PIMM concept deploys a 1.6 mm thick 50 mm diameter slotting cutter rotating at high speed (17 000 rpm) mounted on a computer controlled X-Y carriage (Fig. 1). The profile required on the timber is generated by the X-Y slide movement from a 'soft' profile stored in computer memory. The profile is generated in a simple CAD system built into the user interface or via a proprietary CAD system as desired. The timber to be profiled is indexed in the feed direction after each pass of the slotting

cutter by an amount equal to the desired surface wave pitch; normally 1-2 mm. The work detailed in Taşcıoğlu and Jackson (2005) showed typical output speeds and profiling accuracies attained first by simulation and then by a test rig facility. The time taken for the PIMM to execute one pass of the profiled section is typically 1 second, but this is influenced by the size and features of the profile to be produced. The rate of production from the PIMM is influenced by the 'contouring speed' which is the time taken for the cutter to travel from one side of the timber to the other along the width while cutting and the 'profile quality' in terms of geometric accuracy and surface waviness.

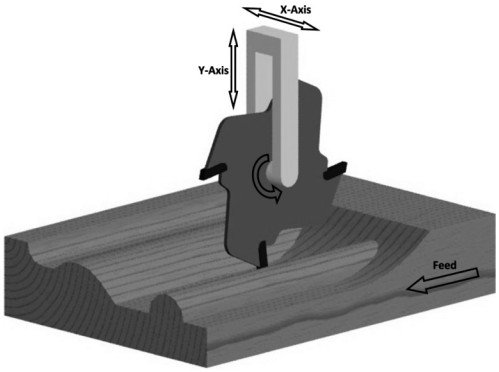

Fig. 1: PIMM Concept

In all of the dynamic machining processes, the nature of the cutting forces must be understood before accurate analysis of the production in terms of cost, quality and efficiency. It is not intended for this work to present a wide view of the cutting forces encountered during wood machining. This has been treated in detail by Kivimaa (1950), Walker (1957) and others over the last 50 years. Previous research in Kivimaa (1950) reports the behavior of cutting forces for various types of timbers and machining conditions. Although this work dates back more than fifty years, it is still the most comprehensive investigation in woodworking forces and is referred by most, if not all, of the woodworking researchers dealing with the cutting forces.

The aim of this paper is to investigate the nature of material removal and cutting power requirement in PIMM operation. For that, firstly, chip severing phenomena is described and the factors affecting the cutting forces in rotary wood machining are surveyed. Then, the nature of material removal and the influences of PIMM's machining parameters on cutting forces are theoretically investigated. Finally, purpose designed cutting power measurement setup is explained and experiment results are discussed.

Cutting Forces in Rotary Wood Machining

To separate a chip from a piece of wood, a certain force F must be applied to the tool. This force should be bigger than the cohesion of the wood material and it is the result of several forces. These are, force from the bending of fibers, shearing force and the friction force on the faces of the tool (Aguilera and Martin 2001). The total cutting force F can be divided into two components as shown in Fig. 2. Tangential force component F_t acts parallel to the movement direction of the cutting tool and the radial force component F_n is normal to this. F_t is considered to be the main component and it determines the energy consumption. Depending on the direction of the cutting force F, the F_n may be directed either towards or away from the wood surface. In the former case the component F_n is termed positive, and in the latter case negative (Fig. 2).

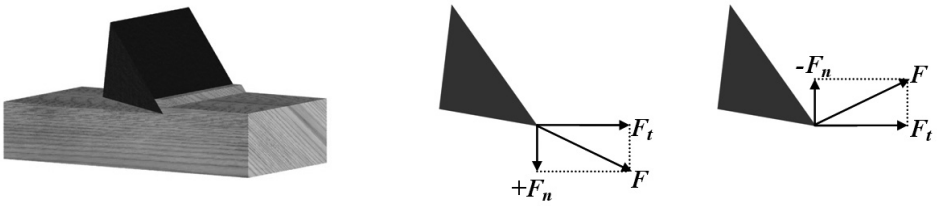

Fig. 2: Cutting force F and its components Ft and Fn

Cutting forces are influenced by various machine and tooling parameters in rotary machining, such as the radius of the cutting circle *r*, cutting depth *d*, feed speed *f*, cutting speed *v*, cutter rake angle α and mean chip thickness δ_m. These are illustrated in Fig. 3.

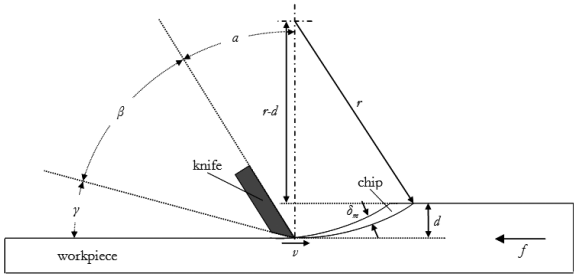

Fig. 3: Rotary chip cutting

The following is a summary of the influence of machine, cutting tool and workpiece variables on cutting forces.

Cutting direction

Due to the anisotropic and cellular structure of wood, the cutting forces are influenced by the cutting direction. The cutting directions in the industry are determined by knife movement direction, cutting surface plane and direction of grain. The three main cutting directions are shown in Fig. 4.

Generally, the magnitude of the main cutting force is the lowest in the C (veneer) direction. The A (crosscut) direction produce the highest main cutting forces because the wood is required to be failed in tension parallel to the grain (Woodson and Koch 1970). In the B (planing) direction, both the cutting surface and knife movement are parallel to the grain and the magnitude of forces are in between the A and C directions.

The B direction is reported here after since this is the one where the planing and moulding processes are carried out.

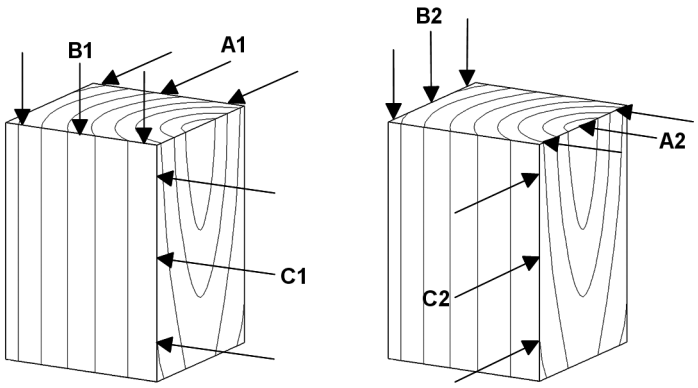

Fig. 4: Main cutting directions in wood machining

Width of cut

It is well established that the cutting forces are directly proportional to the width of cut, provided that the cutting edge always overlaps the workpiece. Most of the authors have reported the cutting forces per unit width of cutter/workpiece engagement.

Cutting speed

In practice, the cutting speed of woodworking tools can be from less than 1 $m.s^{-1}$ to more than 125 $m.s^{-1}$. However, there is no published work which investigates the whole range for cutting forces.

In Kivimaa (1950), tests carried out throughout the range 2.5 $m.s^{-1}$ – 50 $m.s^{-1}$. A work sharp knife having rake angle α = 35° and clearance angle γ = 10° was used to sever chips with an average thickness of δ_m = 0.1 mm from Finnish Birch (11 % moisture content) workpieces. It was reported that no change in tangential or normal cutting forces can be detected.

Tests reported in Walker (1957) are for a range of cutting speeds from 5 $m.s^{-1}$ to 35 $m.s^{-1}$. Chips with δ_m = 0.125 mm were severed from sycamore and beech specimens (12 % moisture content). The cutter rake angle was α = 30°. The results are averaged over five repeat tests and results show that cutting speed has little, if any, influence on the magnitude of cutting forces.

According to (Costes and Larricq 2002), when cutting speed was increased from 15 $m.s^{-1}$ to 150 $m.s^{-1}$ an additional amount of force due to acceleration has to be taken into account. This additional force is almost proportional to the square of the cutting speed and can be assimilated to an inertia force component of chip on the rake face. As a result, the higher the speed is, the greater the acceleration component. However, for turning and sawing, cutting speed contribution on total forces seems to be low and, in any cases, is less than 10 %.

In Huang and Chen (1998) and Huang et al. (2003), oblique wood cutting is performed with a rotting disc cutter. It was reported that the specific cutting energy, which is the work required per unit volume of cut, tends to increase as the rotating speed of the disc cutter increases. This implies that the increase in the circumference speed of the cutter would increase the required energy, most of which would transform into heat and cause a rise in the temperature of the cutting knife.

In the light of the previous work, it can be concluded that the effect of the cutting speed on the cutting forces is negligible. On the other hand, many authors agree that higher cutting speed gives better surface quality. The common explanation is that the speed increase acts as if the wood fibers' inertia and stiffness have been increased. As a result fiber severance is cleaner and surface quality is better (Costes and Larricq 2002, Jackson 1986).

Timber properties and condition

Kivimaa (1950) investigated the main cutting force on 21 different wood species ranging from Balsa wood (0.15 specific gravity) to indian ebony (1.2 specific gravity). A cutter with a rake angle of α = 35° and clearance angle of γ =10° was used to severe 0.1 mm thick chips from specimens of 11 % moisture content. The results show that the main cutting force increases with density and, one might expect a times two increase in the magnitude of the cutting force depending on the wood species.

Aguilera et al. (2000) and McKenzie et al. (2001) reports cutting force tests on MDF boards having layers of different densities by using CNC routers and piezo-electric dynamometers. The results are in accordance with the ones obtained in (Kivimaa 1950). Greater specific gravity substantially means less cell cavities and more cell walls in the wood; consequently, the force required to move the tool must also be greater (Eyma et al. 2001).

Temperature and moisture content of the wood has little effect on the cutting forces. As the temperature of the timber increases, a slight decrease occurs in the cutting resistance. Also, increasing moisture content over 10 % results in decreased cutting forces.

Cutter geometry and condition of the cutter edge

As in metal working, cutter geometry has a significant influence on the nature of the cutting forces developed during rotary woodworking. Cutter geometry parameters rake angle α, sharpness angle β and, clearance angle γ can be seen in Fig. 3.

Kivimaa (1950) reports on the influence of cutter rake angle α being varied from -3° to +60° while keeping all other factors constant, with the exception to the sharpness angle β which is clearly interrelated to α and γ (Fig. 3). The results show that the rake angle has a significant effect on both the tangential and normal cutting forces. Rake angles smaller than 20° cause both cutting force components to increase. This is more significant at greater chip thicknesses.

Further inspection of the results in (Kivimaa 1950) reveals that the tangential cutting force Ft is always positive and increases with decreasing rake angle. Whereas, the normal force Fn is seen to be negative for rake angles between α = 20° and α = 50°; and can be considered as pulling the workpiece into the cutterhead. According to (Jackson 1986), when the cutter engages the workpiece, it pushes the workpiece away and rubs over the surface until it can 'bite' and start to cut, at which point the normal force Fn becomes negative and the cutter starts pulling the workpiece into the cutterhead. For smaller rake angles (i.e. α < 20°), it is more difficult for the cutter to 'bite' the workpiece, and therefore, extended rubbing phase results in positive normal force. Increasing the rake angle further than α = 50°, while keeping the clearance angle γ constant, results in very small sharpness angles β and the cutting edge gets duller due to its failure to stand the force directed to it. Dull cutting edge cannot 'bite' the workpiece and positive normal forces occur due to extended rubbing.

Another investigation (Walker 1957), where the cutting speed and chip thickness are 35 $m.s^{-1}$ and 0.125 mm respectively, shows that reducing the rake angle from 30° to 15° increased the tangential force from 5 $N.mm^{-1}$ to 10 $N.mm^{-1}$ and the radial force from 0 to 3.5 $N.mm^{-1}$.

In another set of experiments, reported in Kivimaa (1950), the clearance angle γ is varied between 2° and 35° while keeping all other factors constant, with the exception to the sharpness angle β. As γ is increased, with constant α, the cutting forces are seen to decrease until a value of γ = 15° is reached at which point a significant change occurs in the cutting force curves, and forces further increase with γ. This is explained by observing a critical sharpness angle β_{crit} below which microscopic chipping of the cutting edge occurs after a small number of engagements of the cutter with the workpiece.

Consequently, there exists a compromise between large rake and clearance angles in order to

keep the sharpness angle greater than β_{crit}. It appears therefore, that a maximum rake angle of 35°, with sharpness angle of 45° and clearance angle of 10° is a reasonable compromise at this extreme.

Chip thickness

Chip thickness, together with cutter geometry is the most significant parameter affecting the cutting forces. Kivimaa (1950) studied the influence of chip thickness by using both work-sharp and dull cutters in order to form some kind of conception of the limits within which the force components vary when the tool gradually dulls during work. Nine different thicknesses from 0.0125 mm to 0.5 mm were employed.

First of all, it is shown that dulling of the knife increases cutting forces irrespective of chip thickness. This increase is greater at thinner chips. Within the chip thickness range from 0.025 mm to 0.5 mm, tangential force curves are almost linear. Extensions of the Ft lines do not run through the origin but bisects the ordinate axis at a point above the origin. It is explained that the power required for cutting wood is needed for two different purposes. One part of the power is required for affecting the cutting proper (i.e. shearing) and remains constant while chip thickness varies. This part mainly depends on knife sharpness. The other part is needed for deforming the severed chips still resting against the knife face and, for this reason, depends largely on chip thickness and is, within a certain range, almost a linear function. Moreover, it also depends substantially on the rake angle of the knife, which determines the degree of deformation and type of injury done to the chips.

Upcutting and downcutting

Over the years, the relative merits of upcutting and downcutting have been investigated by some researchers on different wood machining processes. Generally, downcutting generates greater cutting forces and requires more power, up to 25 %, due to increased average chip thickness (Aguilera and Martin 2001, Jackson et al. 2002, Huang et al. 2003).

The work presented in Schajer and Wang (2001) and Schajer and Wang (2002) discuss the influence of up and downcutting on circular saw cutting stability. The results show that upcutting improves sawing accuracy due to reduced saw deflection resulting from the sideways component of the reaction force on the saw.

Down-cutting also have a number of significant difficulties to overcome such as control of timber to prevent 'snatch' occurring and extraction of wood chips which exit in the feed direction (Jackson 1986).

Theoretical investigation of material removal in PIMM

The aim of this section is to predict cutting forces and cutting power in the PIMM process.

Due to the traverse motion of the cutting disc along the workpiece width, it is assumed that the side of the cutting tool as well as the tip perform cutting. Consequently, the cutting forces were estimated for two cutting edges (i.e. side and tip) and then combined. Fig. 5 illustrates the cutting force components acting on the cutting edges, where F_{st} and F_{sn} are the tangential and normal components acting on the side of the tool and F_{tt} and F_{tn} are the forces acting on the tip of the tool.

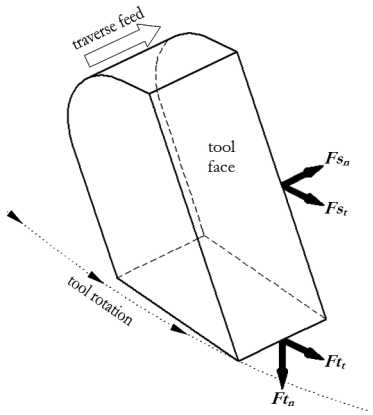

Fig. 5: Forces acting on the tool edges

Fig. 6 shows the cutter-workpiece interaction and the important geometric parameters of the produced chips, where f is the feed increment, d is the depth of cut, c is the chip width and δ_m is the mean chip thickness. Another important parameter, chip length L is the length of the circular section at the bottom of the chip. Chip length L and the mean chip thickness δ_m are calculated by equations (1) and (2) respectively, where r is the cutter radius.

$$L = \cos^{-1}\left(\frac{r-d}{r}\right)\cdot r \tag{1}$$

$$\delta_m = f \cdot \frac{d}{L} \tag{2}$$

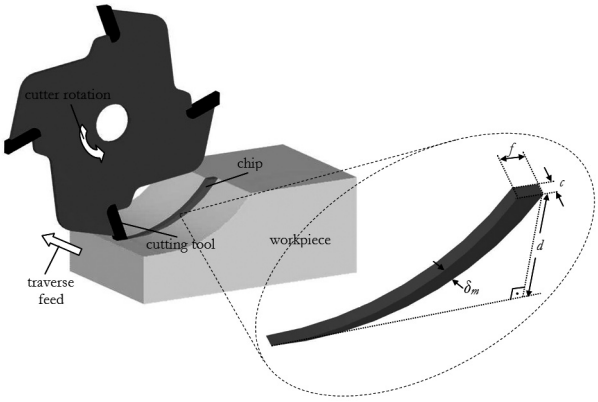

Fig. 6: Cutter–workpiece interaction

At this point; some of the influencing factors, explained in the previous section, can be adapted to PIMM operation while keeping in mind the following assumptions:

Assumption 1: Side and tip edges of a cutter tooth are cutting at the same time.

Assumption 2: Only a single tooth is in contact with the workpiece at any time.

Assumption 3: The ratio of cutting speed to traverse speed is great enough, such that, the chip width stays constant throughout the cutter tooth workpiece engagement.

It can be understood from Fig. 4 and 5 that when one of the edges (i.e. side or tip) is cutting on B1 direction, the other edge cuts on B2 direction and vice versa. Therefore, for both edges, conditions of B direction are valid.

In PIMM, the cutting speed can only be changed by changing the spindle speed. In the previous section, it was concluded that the effect of the cutting speed on the cutting forces is negligible for conventional wood machining processes. However in PIMM, due to the traverse motion of the cutter, the cutting speed has an indirect, yet significant, influence on the cutting forces. Increasing the cutting speed, while keeping the traverse speed constant, increases the number of cutter-workpiece engagements per unit length along the traverse direction. Consequently, teeth of the cutter sever chips with smaller width and hence result in smaller forces. This is formulated in equations (3) and (4), where, n_p is the number of cutter-workpiece engagements per pass, n is the number of cutter teeth, ω is cutting speed in rpm, t is the pass time in s, and c and w are chip and workpiece widths in mm respectively.

$$n_p = \frac{\omega}{60} \cdot n \cdot t \tag{3}$$

$$c = \frac{w}{n_p} \tag{4}$$

For the tip of the cutter, width of cut (i.e. width of cutter-workpiece engagement) at any given time is equal to the chip width c (Fig. 6). On the other hand, chip thickness increases from 0 to f during a single cut and its mean value δ_m is used to characterize this parameter.

When the side of the cutter is considered, the chips have constant thickness which is equal to the dimension c. This time the width of cut increases from 0 to f and, δ_m value can be considered as the mean cutting width for the side of the cutter (Fig. 6).

At this point, equation (5) can be used to calculate the total tangential force component Ft from the 'per unit width' cutting force data of previous studies, such as (Kivimaa 1950).

$$F_t = Ft_t \cdot c + Fs_t \cdot \delta_m \tag{5}$$

Feed increment f is directly proportional to the mean chip thickness δ_m, therefore an increase results in greater cutting forces.

Decreasing the pass time t (i.e. increasing the traverse speed) causes smaller number of chips, having greater chip widths, to be produced. This results in greater cutting forces.

Increasing the depth of cut d increases the chip length L as well as the mean chip thickness δ_m. Consequently, results in greater cutting forces.

Increasing the cutter radius r results in greater chip length L, smaller mean chip thickness δ_m, and hence, smaller cutting forces.

Under the assumption 2, increasing the number of cutter teeth causes more chips to be produced but with smaller chip widths, and therefore, results in smaller cutting forces. This tendency is the same as in the case of increased spindle speed.

Alternatively, if the number of cutter teeth is increased such that the assumption 2 cannot be valid (i.e. more than one teeth lies along the chip length *L*), then according to the assumption 3 only the front tooth produces a chip.

Hence, the assumption 2 can be cancelled by defining a variable n_L (6) for the number of teeth on the portion of the cutter circumference, which is equal to the chip length; and redefining the chip width (7).

$$n_L = \frac{L}{2 \cdot \pi \cdot r} \cdot n \tag{6}$$

$$c = \begin{cases} \dfrac{w}{n_p} & n_L \le 1 \\ \dfrac{w}{n_p / n_L} & n_L > 1 \end{cases} \tag{7}$$

If $n_L \le 1$ then a chip is severed at each engagement between the cutter teeth and the workpiece. On the other hand, when $n_L > 1$; although n_p teeth runs over the workpiece, only n_p/n_L chips are severed.

Tab.1 generally summarizes the influence of the PIMM machining parameters on the cutting forces.

Tab. 1: Influence of the PIMM machining parameters on cutting forces

parameter		**Increase in parameter**	**Decrease in parameter**
cutter radius	r	low F	high F
number of teeth	n	low F	high F
rake angle	α	low F	high F
cutting speed	ω	low F	high F
workpiece width	w	no-change	no-change
depth of cut	d	high F	low F
feed increment	f	high F	low F
pass time	t	low F	high F

To estimate the cutting power, firstly, the work W_c along the direction of motion in order to severe one chip is calculated (8). Then, the number of chips severed in one second *n'* is computed (9). Finally, the estimated power Pe is found by multiplying W_c and *n'* (10).

$$W_c = F_t \cdot L \tag{8}$$

$$n' = \begin{cases} \dfrac{\omega \cdot n}{60} & n_L \le 1 \\ \dfrac{\omega \cdot n}{60 \cdot n_L} & n_L > 1 \end{cases} \tag{9}$$

$$P_e = W_c \cdot n' \tag{10}$$

The estimated value only includes the power required for material removal and does not contain the effects of possible friction. Experimental investigations, presented in the next section, provide better understanding of the cutting power requirements.

MATERIAL AND METHODS

Cutting power measurements were performed on a purpose designed experiment setup (Fig. 7), in which, timber specimens are fed towards a rotating cutter from the side and a single pass along the timber width is performed with a constant depth of cut. The setup comprises of three main parts: frame, feed drive and cutter assembly.

The feed drive features a DC motor driven ballscrew and precision linear guides, and it provides longitudinal movement up to 125 mm.s^{-1}. Prior to cutting, the whole feed drive is moved towards the cutter assembly in order to set the feed increment *f*, and the motor speed is adjusted to achieve the desired pass time *t*.

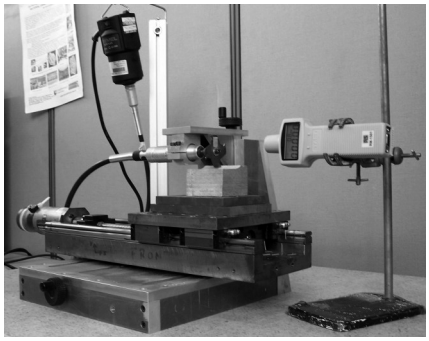

Fig. 7: Experiment setup

The cutter, which is attached to a collet, is driven by a Dremel Multi-Tool via a flexible shaft. The Dremel motor is a 250 W, 220V AC motor and its speed can be adjusted manually in the range of 5000 – 22000 rpm. The cutting speed ω is measured with a non-contact optical tachometer having 1 s sampling rate. Prior to cutting, the cutter assembly can be moved in vertical direction to set the desired depth of cut d. A 4-teeth slotting saw with 1.6 mm kerf width and 50.8 mm diameter, and a 20-teeth circular saw with 1 mm kerf width and 85 mm diameter were used in the experiments.

Initially the setup was designed to measure the cutting forces directly with a three-axis load cell, attached to the feed table and carrying a timber specimen. Series of tests had been performed;

however, meaningful cutting force data could not be acquired in any of the three directions. As it can be understood from the previous sections, the magnitudes of the cutting forces are very small (i.e. in the order of a few Newtons maximum). These small forces could not be detected among the vibration of the setup and the electrical noise of the available equipment (i.e. charge amplifiers). Design and manufacture of a special purpose load cell was outside the scope of this research work; consequently, the load cell arrangement was not used.

As an alternative approach, it was decided to derive the cutting power and forces from the power input to the cutter motor. Timber specimens were screwed directly to the feed table and an AC watt-meter, which is capable of measuring the average power in 1 s intervals, was connected between the cutter motor and the mains socket. Similar methods, utilizing a watt-meter, are reported in Aguilera and Martin (2001), Aguilera et al. (2000), Huang et al. (2003). The findings show that, very high correlation exists between the power calculated from measured cutting forces and the power measured directly with a watt-meter; and this correlation permits estimation of cutting forces for given machining conditions. Fig. 8 shows the schematic of the final experiment setup.

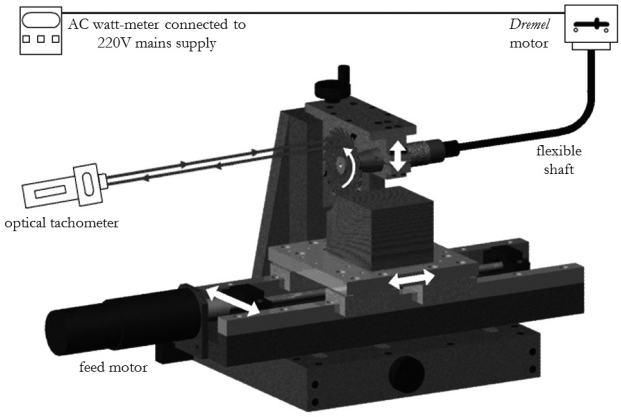

Fig. 8: Experiment setup schematic

The following steps show the procedure repeated for each test:
Step 1: Set depth of cut d by adjusting the cutter assembly position.
Step 2: Set feed increment f by adjusting the feed drive position.
Step 3: Set pass time t by adjusting the feed motor speed.
Step 4: Set cutter idling speed ω_{idle}.
Step 5: Record power consumption of the idling cutter motor P_{idle}.
Step 6: Switch on the feed motor.
Step 7: While cutting, record cutter speed ω, and power consumption of the cutter motor P_{total}.
Step 8: When cutting ends, switch off feed and cutter motors.

Before the timber is fed to the cutter, idling power consumption P_{idle} of the cutter motor, at the desired idling speed ω_{idle}, is read from the watt-meter. Consequently; the torque resulting from the rotating inertias (i.e. rotor, flexible shaft, and cutter) and friction, is figured out from equation (11).

$$T_{idle} = \frac{P_{idle}}{\omega_{idle}} \tag{11}$$

When the cutting starts, the cutter speed drops to a lower value and stays there until the cutting ends. This is due to the cutter motor having no means of real-time control to compensate the cutting torque. Therefore, the cutter speed ω and the total power consumption of the cutter motor P_{total} are read; and the total torque is calculated (12).

$$T_{total} = \frac{P_{total}}{\omega} \tag{12}$$

$$T = T_{total} - T_{idle} \tag{13}$$

To find the cutting torque (i.e. torque required for severing chips from workpiece), the idling torque T_{idle} is subtracted from the total torque T_{total} (13). From the cutting torque, cutting power P and total tangential cutting force F_t is calculated by equations (14) and (15) respectively, where r is the cutter radius.

$$P = \omega \cdot T \tag{14}$$

$$F_t = \frac{T}{r} \tag{15}$$

Tab. 2: Experiment series

Series #	Cutter						Workpiece		Machine				
	r	n	α_t	γ_t	αs	γs	w	s_{12}	f	d	t	ω_{idle}	P_{idle}
	(mm)		(°)	(°)	(°)	(°)	(mm)		(mm)	(mm)	(s)	(rpm)	(W)
1	25.4	4	15	10	0	10	70	0.55	1	5	2	17000	105
2	25.4	4	15	10	0	10	70	0.55	2	5	2	17000	105
3	25.4	4	15	10	0	10	70	0.55	3	5	2	17000	105
4	25.4	4	15	10	0	10	70	0.55	1	5	3	17000	105
5	25.4	4	15	10	0	10	70	0.55	2	5	3	17000	105
6	25.4	4	15	10	0	10	70	0.55	3	5	3	17000	105
7	25.4	4	15	10	0	10	70	0.55	1	5	4	17000	105
8	25.4	4	15	10	0	10	70	0.55	2	5	4	17000	105
9	25.4	4	15	10	0	10	70	0.55	3	5	4	17000	105
10	42.5	20	10	10	0	10	70	0.55	1	5	3	13500	106.5
11	42.5	20	10	10	0	10	70	0.55	2	5	3	13500	106.5
12	42.5	20	10	10	0	10	70	0.55	1	10	3	13500	106.5
13	42.5	20	10	10	0	10	70	0.55	2	10	3	13500	106.5
14	42.5	20	10	10	0	10	70	0.55	1	15	3	15000	106.5

Measurements were carried out in 14 different series, each of which consisted of five identical tests. The arithmetic means of the obtained ω and P_{total} values were used in further calculations.

70 mm wide Meranti wood specimens having specific gravity s_{12} = 0.55 were used as specimens and two different off-the-shelf cutters were used. Cutter, workpiece and machine parameters of the test series are listed in Tab. 2.

RESULTS AND DISCUSSION

Tab. 3 shows the measured and calculated results for the test series. In the experiment series 1 to 9, n_L = 0.41 and this value can also be interpreted as; in one revolution of the cutter, only 41 % of the time the cutter is in contact with the workpiece (i.e. cutting). The rest of the time (i.e. 59 %) the cutter is rotating freely, therefore, cutting force is 0 N. The actual cutting force and torque change periodically between zero and a maximum value. The values listed in Tab. 3, which are calculated by equations (13) and (15), represent the average cutting force and torque over time. Consequently; the maximum force and torque values, which occur while the cutter is actually cutting, is found by dividing the average values in Tab. 3 by n_L.

Tab. 3: Experiment results

Series #	Measured		Calculated							
	P_{total} (W)	ω (rpm)	T (Nm)	F_t (N)	P (W)	L (mm)	δ_m (mm)	n_p	n_L	c (mm)
1	120.54	15440	0.016	0.613	25.175	16.21	0.3	2059	0.41	0.034
2	132.40	14380	0.029	1.139	45.582	16.21	0.6	1917	0.41	0.037
3	150.20	13804	0.045	1.769	64.941	16.21	0.9	1841	0.41	0.038
4	118.56	15724	0.013	0.513	21.439	16.21	0.3	3145	0.41	0.022
5	134.44	14613	0.029	1.137	44.183	16.21	0.6	2923	0.41	0.024
6	146.76	13728	0.043	1.697	61.971	16.21	0.9	2746	0.41	0.025
7	115.58	16007	0.010	0.392	16.711	16.21	0.3	4267	0.41	0.016
8	130.12	14981	0.024	0.943	37.589	16.21	0.6	3995	0.41	0.018
9	137.80	14413	0.032	1.272	48.777	16.21	0.9	3844	0.41	0.018
10	123.76	12322	0.021	0.484	26.552	20.8	0.2	12322	1.56	0.009
11	146.86	10795	0.055	1.284	61.696	20.8	0.5	10795	1.56	0.010
12	142.80	11014	0.048	1.140	55.905	29.76	0.3	11015	2.23	0.014
13	190.20	9883	0.108	2.551	112.229	29.76	0.7	9884	2.23	0.016
14	173.80	9871	0.093	2.184	95.927	36.85	0.4	9871	2.76	0.020

Tab. 4 lists the experiment results with corrected torque and force values due to $n_L < 1$. For the experiment series with $n_L > 1$, continuous application of force exists, hence correction is not required.

Tab. 4: Experiment results with corrected torque and force values

Series #	Measured		Calculated							
	P_{total} (W)	ω (rpm)	T (Nm)	F_t (N)	P (W)	L (mm)	δ_m (mm)	n_p	n_L	c (mm)
1	120.54	15440	0.039	1.495	25.175	16.21	0.3	2059	0.41	0.034
2	132.40	14380	0.071	2.778	45.582	16.21	0.6	1917	0.41	0.037
3	150.20	13804	0.110	4.315	64.941	16.21	0.9	1841	0.41	0.038
4	118.56	15724	0.032	1.251	21.439	16.21	0.3	3145	0.41	0.022
5	134.44	14613	0.071	2.773	44.183	16.21	0.6	2923	0.41	0.024
6	146.76	13728	0.105	4.139	61.971	16.21	0.9	2746	0.41	0.025
7	115.58	16007	0.024	0.956	16.711	16.21	0.3	4267	0.41	0.016
8	130.12	14981	0.059	2.300	37.589	16.21	0.6	3995	0.41	0.018
9	137.80	14413	0.078	3.102	48.777	16.21	0.9	3844	0.41	0.018
10	123.76	12322	0.021	0.484	26.552	20.8	0.2	12322	1.56	0.009
11	146.86	10795	0.055	1.284	61.696	20.8	0.5	10795	1.56	0.010
12	142.80	11014	0.048	1.140	55.905	29.76	0.3	11015	2.23	0.014
13	190.20	9883	0.108	2.551	112.229	29.76	0.7	9884	2.23	0.016
14	173.80	9871	0.093	2.184	95.927	36.85	0.4	9871	2.76	0.020

Most of the previous work in literature is aimed at measuring instantaneous cutting forces directly. Some of them employed a wattmeter based power measurement method, similar to the one presented here, and shown the close correlation between the directly measured forces and the forces derived from power measurements. In conventional moulding process, where only the tip edge of the cutter is in contact with the workpiece, the greatest influence on the magnitude of cutting forces is from cutter geometry parameters and chip thickness. Although the order of magnitude and the tendencies of the cutting forces in this work are in agreement with the literature (Aguilera and Martin 2001, Huang et al. 2003, Kivimaa 1950) there is no means for direct comparison since the cutter and chip parameters of this work are impractical for conventional moulding and not reported previously.

Figs. 9, 10 shows bar charts of measured cutting power for experiment series 1 to 9 and 10 to 14 respectively. The numbers on the bars indicate the experiment series number. As expected, more power is consumed at deeper cuts, higher feed increments, and lower pass times.

Greater feed increments increase PIMM's production rate but require more cutting power. On the other hand, feed increment is also equal to the surface wave pitch and higher quality surfaces

require smaller wave pitches (normally 1-2 mm). Consequently, there is not a trade-off between cutting power and quality.

Pass time also affects the production rate directly, but this time there is a trade-off. Experiments with the target pass time of 1 s could not be performed due to the limitations of the measuring hardware. However, examining the results of the experiment series 1 to 9, one would expect around 70 W for 3 mm feed increment, 50 W for 2 mm and 30 W for 1 mm, without changing any other parameter.

Also, PIMM requires up to 20 mm deep cuts to be able to produce majority of the profiles in the market. Fig. 10 b shows that, starting from 5 mm depth of cut and increasing 5 mm at a time, the cutting power increases in a geometric sequence with a common ratio of 2. Hence, it is valid to say that 20 mm deep cuts require eight times more power than 5 mm ones.

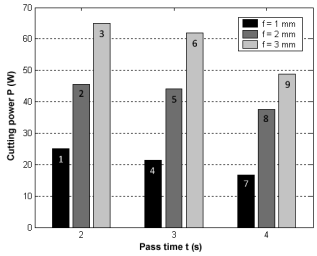

Fig. 9: Measured power for experiment series 1 to 9

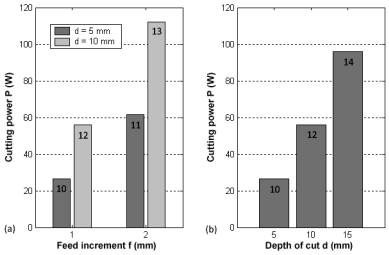

Fig. 10: Measured power for experiment series 10 to 14

CONLUSIONS

The PIMM allows production of virtually any moulding profile with only a single cutting tool. Previous work proves the viability of the new concept but mainly concentrates on the generation of the profiles. The work presented in this paper approached the concept from wood machining perspective in order to determine the cutting power requirement. Firstly, chip severing phenomena is described and the factors affecting the cutting forces in rotary wood machining are surveyed. Then, the nature of material removal and the influences of PIMM's machining parameters on cutting forces are theoretically investigated. Finally, purpose designed cutting power measurement setup is explained and experiment results are discussed. In the experiments, two different off-the-shelf cutters, namely a 4-teeth 50.8 mm diameter slotting saw and a 20-teeth 85 mm diameter

circular saw, were used. It can be concluded that, with the cutters used, the peak cutting power required to produce majority of the profiles in the market with good surface quality at the target pass time of 1 s is less than 500 W. This value can be lowered by using cutters with larger rake angles. However, considering the small kerf widths of the cutters, larger rake angles make the cutters more fragile and therefore more vulnerable to dulling. Further work should be focused on the design and optimization of a dedicated cutter for the PIMM.

REFERENCES

1. Aguilera, A., Meausoone, P. J., Martin, P., 2000: Wood material influence in routing operations: the MDF case. Holz als Roh- und Werkstoff 58: 278-283
2. Aguilera, A., Martin, P., 2001: Machining qualification of solid wood of *Fagus silvatica* L. and *Picea excelsa* L.: cutting forces, power requirements and surface roughness. Holz als Roh- und Werkstoff 59: 483-488
3. Costes, J. P., Larricq, P., 2002: Towards high cutting speed in wood milling. Ann. Forest Science 59: 857-865
4. Eyma, F., Meausoone, P. J., Martin, P., 2001: Influence of the transitional zone of wood species on cutting forces in the router cutting process (90-0). Holz als Roh- und Werkstoff 59: 489-490
5. Huang, Y. S., Chen, S. S., 1998: Oblique wood cutting with a rotating disc cutter. Taiwan Journal of Forest Science 13(4): 301-307
6. Huang, Y. S., Chen, S. S., Hwang, G.S., Tang, J. L., 2003: Peripheral milling properties of compressed wood manufactured from planted China-fir. Holz als Roh- und Werkstoff 61: 201-205
7. Huang, Y. S., Chen, S.S., Tang, J. L., 2003: Analysis of rotating disc cutting of wood. Taiwan Journal of Forest Science 18(4): 263-271
8. Jackson, M. R., 1986: Some effects of machine characteristics on the surface quality of planed and spindle moulded wooden products, Dissertation, Leicester Polytechnic
9. Jackson, M. R., Neumayer, R., Parkin, R. M., Brown, N., 2000: Profile independent wood moulding machine dynamic model and control system. In: Proc. Of the 7th Mechatronics Forum International Conference, Pergamon, Atlanta, USA
10. Jackson, M. R., Parkin, R. M., Brown, N., 2002: Waves on wood. Proceedings of the IMechE, Part B: Journal of Engineering Manufacture 216: 475-497
11. Jackson, M. R., Tascıoglu, Y., 2007: Profile Independent Wood Moulding Machine II. In: Proc. of the 18th International Wood Machining Seminar, Vancouver, Canada
12. Kivimaa, E., 1950: Cutting force in wood working, Dissertation, University of Helsinki
13. McKenzie, W. M., Ko, P., Cvitkovic, R., Ringler, M., 2001: Towards a model predicting cutting forces and surface quality in routing layered boards. Wood Science and Technology 35: 563-569
14. Schajer, G. S., Wang, S.A., 2001: Effect of workpiece interaction on circular saw cutting stability I: Theoretical background. Holz als Roh- und Werkstoff 59: 388-393
15. Schajer, G. S., Wang, S.A., 2002: Effect of workpiece interaction on circular saw cutting stability II: Experimental results. Holz als Roh- und Werkstoff 60: 48-54
16. Tascıoglu, Y., Jackson, M.R., 2004: Design alternatives for a novel wood moulder. In: Proc. of the 9th Mechatronics Forum International Conference, Atilim University Publications, Ankara, Turkey, Pp. 833-840

17. Tascıoglu, Y., Jackson, M. R., 2005: Profile independent wood moulding machine. In: Proc. of the 17th International Wood Machining Seminar, Retru-Verlag, Germany, Pp 337-345
18. Walker, K. J. S., 1957: Cutting speed and cutting forces. Wood, 22
19. Woodson, G. E., Koch, P., 1970: Tool forces and chip formation in orthogonal cutting of loblolly pine. U.S. Department of Agriculture, Forest Service Research Paper SO-52

Yiğit Taşcioğlu
Tobb University of Economics and Technology
Department of Mechanical Engineering
Sogutozu
06560 Ankara
Turkey
E-mail: ytascioglu@etu.edu.tr
Tel: +90 312 292 4270

Mike R. Jackson
Loughborough University,
Mechatronics Research Centre
Holywell Building
Holywell Way
Loughborough
Leicestershire, Le11 3uz
Uk
E-mail: m.r.jackson@lboro.ac.uk
Tel: +44 1509 22 75 70